



Contents lists available at ScienceDirect

# Spectrochimica Acta Part A: Molecular and Biomolecular Spectroscopy

journal homepage: [www.elsevier.com/locate/saa](http://www.elsevier.com/locate/saa)

## Molecular characteristics of a fluorescent chemosensor for the recognition of ferric ion based on photoresponsive azobenzene derivative

Zhen Chi, Xia Ran<sup>\*</sup>, Lili Shi, Jie Lou, Yanmin Kuang, Lijun Guo<sup>\*</sup>

Institute of Photobiophysics, School of Physics and Electronics, Henan University, Kaifeng, PR China

### ARTICLE INFO

#### Article history:

Received 31 January 2016

Received in revised form 24 June 2016

Accepted 19 July 2016

Available online 20 July 2016

#### Keywords:

Azobenzene derivatives

Fluorescence sensor

Ferric ion

Photoisomerization

### ABSTRACT

Metal ion recognition is of great significance in biological and environmental detection. So far, there is very few research related to the ferric ion sensing based on photoresponsive azobenzene derivatives. In this work, we report a highly selective fluorescent “turn-off” sensor for  $\text{Fe}^{3+}$  ions and the molecular sensing characteristics based on an azobenzene derivative, N-(3,4,5-octanoxypyphenyl)-N'-4-[(4-hydroxyphenyl)azophenyl]1,3,4-oxadiazole (AOB-t8). The binding association constant was determined to be  $6.07 \times 10^3 \text{ M}^{-1}$  in ethanol and the stoichiometry ratio of 2:2 was obtained from Job's plot and MS spectra. The AOB-t8 might be likely to form the dimer structure through the chelation of ferric ion with the azobenzene moiety. Meanwhile, it was found that the photoisomerization property of AOB-t8 was regulated by the binding with  $\text{Fe}^{3+}$ . With the chelation of  $\text{Fe}^{3+}$ , the regulated molecular rigidity and the perturbed of electronic state and molecular geometry was suggested to be responsible for the accelerated isomerization of AOB-t8 to UV irradiation and the increased fluorescence lifetime of both *trans*- and *cis*-AOB-t8-Fe(III). Moreover, the reversible sensing of AOB-t8 was successfully observed by releasing the iron ion from AOB-t8-Fe(III) with the addition of citric acid.

© 2016 Published by Elsevier B.V.

### 1. Introduction

Metal ion recognition is of significance in supramolecular chemistry and plays an important role for the potential applications in environmental, chemical and biological fields, and a variety of fluorescent sensors of metal ion have been reported in the past decades [1–4]. Chemosensors are compounds demonstrating remarkable changes in their electronic, magnetic or optical properties in binding with specific guests, and have attracted increasing interests in various fields due to the inherent simplicity, highly sensitive and selective features [5,6]. In recent years, a large number of works about detection of  $\text{Pb}^{2+}$ ,  $\text{Zn}^{2+}$ ,  $\text{Cu}^{2+}$ , and  $\text{Hg}^{2+}$  have been reported by monitoring the fluorescence properties of chemosensors [7–15]. In the fields of life science, iron ion is a highly important metal ion for living organisms and plays a significant role in many biochemical processes. The trivalent form of iron is the most abundant essential inhuman body [16], acting as a cofactor in many enzymatic reactions and providing the oxygen-carrying capacity of proteins. The overloading or deficiency of  $\text{Fe}^{3+}$  can induce various disorders with iron trafficking, such as cancer, neurodegenerative and cardiovascular diseases [17,18]. So far, there have been many fluorescent sensors for  $\text{Fe}^{3+}$  reported in recent years [19,20]. However, the development of fluorescent chemosensor with variable conformation for  $\text{Fe}^{3+}$  is still of significant research potential.

Azobenzene and its derivatives are characterized with their photochromic properties because they can undergo photoinduced *trans*–*cis* isomerization [21–23]. In the past decades, they have been widely used as photo-responsive materials, such as liquid crystal, holographic surface relief grating and optical data storage [24–26]. Recently, azobenzene derivatives were presented as a photoswitches by coupling the photoisomerization moiety to regulate the function/structure of numerous biomolecular targets, including proteins, peptides, and nucleic acids *in vitro* and *in vivo* [27,28]. For example, Liang et al. reported that DNA triplex formation was regulated by using *cis*–*trans* isomerization of azobenzene [29]. Wong et al. presented an azobenzene moiety to be used as a multiresponsive end-cap in self-immolative polymer [30]. Samanta and colleagues demonstrated a tetra-ortho-substituted azobenzene compound with the switching properties to red light [31]. However, vanishingly few papers about azobenzene derivatives were reported in the application of fluorescent sensor for transition metals. It would be of considerable significance in developing azobenzene derivatives-based fluorescent sensors for detection ferric ions, especially in environmental and physiological conditions. In this work, we report the sensing characteristics for ferric ion recognition based on an azobenzene derivative (N-(3,4,5-octanoxypyphenyl)-N'-4-[(4-hydroxyphenyl)azophenyl]1,3,4-oxadiazole) (AOB-t8). The photoresponsive AOB-t8 demonstrates a turn-off sensor with high selectivity toward  $\text{Fe}^{3+}$  among 14 metal ions, and possesses a fluorescent “ON–OFF–ON” functional mode via alternately binding  $\text{Fe}^{3+}$  and  $\text{C}_6\text{H}_5\text{O}_3^-$  along with reversible formation/separation of the complex in ethanol. Meanwhile, the isomerization process of AOB-t8 to UV

<sup>\*</sup> Corresponding authors at: School of Physics and Electronics, Henan University, Kaifeng 475004, PR China.

E-mail addresses: [ranxia@henu.edu.cn](mailto:ranxia@henu.edu.cn) (X. Ran), [junegu@henu.edu.cn](mailto:junegu@henu.edu.cn) (L. Guo).

irradiation can be accelerated by coordinating with  $\text{Fe}^{3+}$  ion due to the enhanced molecular rigidity or coplanarity.

## 2. Experimental section

### 2.1. Materials

All the chemicals and reagents were obtained from commercial suppliers and used as received. The solutions of the selected metal ions were prepared from  $\text{MgCl}_2 \cdot 6\text{H}_2\text{O}$ ,  $\text{Co}(\text{NO}_3)_2 \cdot 6\text{H}_2\text{O}$ ,  $\text{KOH}$ ,  $\text{NaOH}$ ,  $\text{Ni}(\text{NO}_3)_2 \cdot 6\text{H}_2\text{O}$ ,  $\text{ZnCl}_2$ ,  $\text{CuCl}_2 \cdot 2\text{H}_2\text{O}$ ,  $\text{HgCl}_2$ ,  $\text{AgNO}_3$ ,  $\text{FeCl}_3 \cdot 6\text{H}_2\text{O}$ ,  $\text{CaCl}_2$ ,  $\text{Al}(\text{NO}_3)_3 \cdot 9\text{H}_2\text{O}$ ,  $\text{La}(\text{NO}_3)_3 \cdot 6\text{H}_2\text{O}$ ,  $\text{Nd}(\text{NO}_3)_3 \cdot 6\text{H}_2\text{O}$ , respectively.

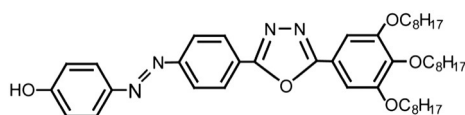
### 2.2. Synthesis and characterization

The molecular structure of *trans*-AOB-t8 is shown in Scheme 1. The synthesis of AOB-t8 was followed the procedure reported in our previous work [32]. Fourier transform infrared (FT-IR) spectra were recorded on a Perkin-Elmer spectrometer with KBr pellets. UV-visible diffuse reflectance spectra were measured using a Perkin-Elmer Lambda 35 spectrometer. Fluorescence spectra in solution were recorded on a Perkin-Elmer LS-55 fluorescence spectrophotometer. The MS spectra were performed on autoflex<sup>TM</sup> speed MALDI-TOF-MS (Bruker). The photoluminescence lifetime measurements were carried out on a home-built lifetime setup (Harp300, Picoquant), coupled with the TCSPC module (time resolution <4 ps) and a broadband pulsed femtosecond laser (Chameleon Ultra II, Coherent Inc.) with the repetition rate of 80 MHz and pulse width of 150 fs, respectively. The 355 nm femtosecond laser was obtained from the secondary harmonic generation with BBO nonlinear crystal and was used as the excitation source, and the fluorescence (>430 nm) was detected with a single photon device (Picoquant, time response <50 ps). The polarization configuration for the excitation and emission was set at the magic angle ( $54.7^\circ$ ), and the impulse response function was measured to be around 50 ps. The UV light for photoisomerization was obtained from a 250 W high-pressure mercury lamp with a 365 nm band-pass filter.

## 3. Results and discussion

### 3.1. Ion response of *trans*-AOB-t8

It is a known fact that azobenzene molecules fluoresce in solution with imperceptible quantum yield. With the molecular grafting of oxadiazole with azobenzene, *trans*-AOB-t8 exhibits a considerable emission and *cis*-AOB-t8 demonstrates an enhanced fluorescence, which can thus be served as the sensing parameter [25]. As shown in Fig. 1(a), the UV-visible spectrum of *trans*-AOB-t8 in ethanol presents an intense absorption at 363 nm, which is attributed to the  $\pi$ - $\pi^*$  transition. The emission maxima at 433 nm in the fluorescence spectrum of *trans*-AOB-t8 can be observed in ethanol with the excitation at 350 nm. In order to investigate the response of *trans*-AOB-t8 to metal ions, the UV/vis absorption measurements of *trans*-AOB-t8 (10  $\mu\text{M}$ ) were performed in the presence of 5 equiv. of 14 different metal ions and the results are shown in Fig. 1(b). It can be found that in the cases of  $\text{K}^+$ ,  $\text{Ni}^{2+}$ ,  $\text{Mg}^{2+}$ ,  $\text{Ca}^{2+}$ ,  $\text{Na}^+$ ,  $\text{Fe}^{3+}$ ,  $\text{Co}^{2+}$ ,  $\text{Ag}^+$ ,  $\text{Hg}^{2+}$ ,  $\text{Zn}^{2+}$ ,  $\text{Cu}^{2+}$ ,  $\text{Al}^{3+}$ ,  $\text{La}^{3+}$  and  $\text{Nd}^{3+}$ , the corresponding absorption spectrum has a very little change. However, the striking difference of absorption from that of free AOB-t8 in ethanol can be observed with the addition of  $\text{Fe}^{3+}$ . Besides the increase of absorbance, an obvious blue-shift of the  $\pi$ - $\pi^*$  absorption maximum from 363 nm to 356 nm is clearly



Scheme 1. The molecular structure of *trans*-AOB-t8.

demonstrated, indicating the perturbation of electronic state and the formation of a new complex with the binding of *trans*-AOB-t8 with  $\text{Fe}^{3+}$  ion [33].

To further explore the characteristics of *trans*-AOB-t8 as an ion-selective fluorescent sensor, the fluorogenic behavior of *trans*-AOB-t8 was investigated with the presence of different metal cations. In the experiments, the concentration of *trans*-AOB-t8 was set as low as 10  $\mu\text{M}$  to avoid the aggregation-caused quenching (ACQ) effect. With the addition of 40 equiv. of  $\text{K}^+$ ,  $\text{Ni}^{2+}$ ,  $\text{Mg}^{2+}$ ,  $\text{Ca}^{2+}$ ,  $\text{Na}^+$ ,  $\text{Fe}^{3+}$ ,  $\text{Co}^{2+}$ ,  $\text{Ag}^+$ ,  $\text{Hg}^{2+}$ ,  $\text{Zn}^{2+}$ ,  $\text{Cu}^{2+}$ ,  $\text{Al}^{3+}$ ,  $\text{La}^{3+}$  and  $\text{Nd}^{3+}$ , the recorded fluorescence spectra are shown in Fig. 2a. It can be found that the presence of  $\text{Fe}^{3+}$  leads to the dramatically quenched fluorescence of *trans*-AOB-t8, while the other test metal ions cause the relatively insignificant change in fluorescence. As a consequence, the color change of *trans*-AOB-t8 solution induced by ferric ion over other metal ions is distinguishable under the illumination of UV lamp (Fig. S1). The highly selective recognition for ferric ion indicates an effective binding of AOB-t8 with  $\text{Fe}^{3+}$ , probably through electron transfer or energy transfer. To further confirm the selectivity for  $\text{Fe}^{3+}$  ion over other metal ions, the metal ion competition experiments were carried out and the results are shown in Fig. 2b. It can be observed that there is nearly no interference for the detection of  $\text{Fe}^{3+}$  from all other metal ions.

In order to gain more insight into the sensor property of *trans*-AOB-t8 toward  $\text{Fe}^{3+}$  ion, the response dependence on the concentration of  $\text{Fe}^{3+}$  ion is shown in Fig. 3. As expected, the fluorescence intensity decreases with the increasing concentration of  $\text{Fe}^{3+}$  ion. The 50% ( $(I_0 - I) / I_0 \times 100\%$ ) of total intensity at the emission maximum can be obtained with the 20 equiv. of  $\text{Fe}^{3+}$  ion, where  $I$  and  $I_0$  represent the fluorescence intensity with and without ferric ion, respectively. On the basis of Stern-Volmer analysis (Fig. S2), the quenching effect can be described with  $(I_0 - I) / I$  versus  $[\text{Fe}^{3+}]$ , where  $I_0$  and  $I$  are the fluorescence intensities in the absence and presence of ferric ion. It can be seen that the Stern-Volmer plot over the  $\text{Fe}^{3+}$  ions concentration ranging from 0 to  $9 \times 10^{-4}$  M demonstrates a linear nature, indicating a static mechanism for the charge transfer between AOB-t8 and ferric ion. The calculated  $K_{SV}$  is of  $6.07 \times 10^3 \text{ M}^{-1}$  for  $\text{Fe}^{3+}$  ion, mainly corresponding to the association constant  $K_s$  for the current sensor [34,35]. To determine the detection limit, the relative fluorescence intensity at 433 nm was plotted as a function of  $\text{Fe}^{3+}$  concentration (Fig. S3), the detection limit based on the definition IUPAC (CDL = 3 Sb/m) [36] is found to be 16.8  $\mu\text{M}$  from 8 blank solutions.

### 3.2. Binding mode of AOB-t8 with $\text{Fe}^{3+}$

In the conjugated AOB-t8, there are several possible sites to chelate with ferric ion, such as -OH,  $\text{N}=\text{N}$  and  $\text{N}-\text{N}$ , which can lead to the fluorescence quenching. To find out the molecular configuration of AOB-t8- $\text{Fe}(\text{III})$  complex, the binding stoichiometry experiments were carried out with a constant concentration of AOB-t8 and  $\text{Fe}^{3+}$ . As shown in Fig. 4, the emission intensity at 433 nm is plotted against the molar fraction of  $\text{Fe}^{3+}$ . From the obtained Job's plot, an inflection point at 0.5 M fraction of  $\text{Fe}^{3+}$  can be clearly observed, indicating a 1:1 or 2:2 ratio between AOB-t8 and  $\text{Fe}^{3+}$  in the inclusion complex [37].

Vibrational spectroscopy can provide information on the coordination bond of metal ions and sensors. To investigate the binding site of AOB-t8 with the metal ions, FTIR spectroscopies of solid AOB-t8 and AOB-t8@ $\text{Co}^{2+}$  and AOB-t8@ $\text{Fe}^{3+}$  were performed. The spectral data in Fig. 5a indicate that the O-H and C-N group stretching vibration modes of AOB-t8 are located at 3427 and 1125  $\text{cm}^{-1}$ , respectively [32]. The peak at 1550  $\text{cm}^{-1}$  is attributed to the C=N stretching vibration of 1,3,4-oxadiazole ring [38]. After adding  $\text{Fe}^{3+}$ , the peak of O-H vibrational mode is slightly shifted to lower wavenumber of 3421  $\text{cm}^{-1}$  and the stretching vibration peak of C-N appears at 1115  $\text{cm}^{-1}$  (Fig. 5c). However, the C=N stretching vibration has no change before and after adding  $\text{Fe}^{3+}$ , indicating that  $\text{Fe}^{3+}$  is not binding with C=N group in oxadiazole moiety. Furthermore, there is almost no

Download English Version:

<https://daneshyari.com/en/article/1229975>

Download Persian Version:

<https://daneshyari.com/article/1229975>

[Daneshyari.com](https://daneshyari.com)